Journal of Materials Chemistry A

Accepted Manuscript

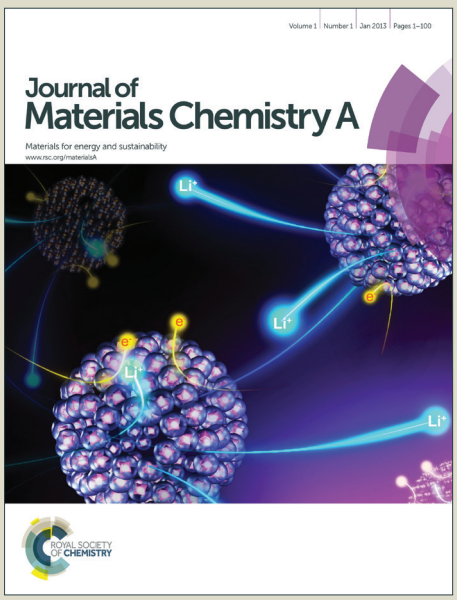

ROYAL SOCIETY OF CHEMISTRY

www.rsc.org/materialsA

Journal of Materials Chemistry A

Cite this: DOI: 10.1039/c0xx00000x

www.rsc.org/xxxxxx

PAPER

Gas uptake, molecular sensing and organocatalytic performances of a multifunctional carbazole-based conjugated microporous polymer

Yuwei Zhang[a], Sigen A[a], Yongcun Zou[b], Xiaolong Luo[b], Zhongping Li[a], Hong Xia[c], Xiaoming Liu[a*], Ying Mu[a]

Received (in XXX, XXX) Xth XXXXXXXXX 200X, Accepted Xth XXXXXXXXX 200X
DOI: 10.1039/b000000x

A multifunctional carbazole-based conjugated microporous polymer MFCMP-1 is successfully prepared by oxidative coupling polymerization using a single monomer and structurally characterized. New three-dimensional π-conjugated polymer framework can be combined permanent microporous, highly luminescent properties and abundant nitrogen activated sites in skeleton. It possesses a large BET surface area of over 840 m^2 g^{-1} with a pore volume of 0.52 cm^3 g^{-1}, and displays high carbon dioxide uptake capacity (up to 3.69 mmol g-1) at 273 K and 1 bar, with good selectivity towards CO_2 over N_2 and CH_4. MFCMP-1 exhibits also strong fluorescent emission at 529 nm after excitation at 380 nm in THF solution and works as a luminescent chemosensor towards hazardous and explosive molecules, such as nitrobenzene, 2-nitrotoluene, 2,4-dinitrotoluene. In addition, MFCMP-1 features a high concentration of Lewis base nitrogen sites on its internal surfaces; it thus acts as a highly efficient recyclable heterogeneous organocatalyst towards Knoevenagel reaction of malononitrile with aromatic, heterocyclic aldehydes, and cyclic ketones. Furthermore, we further highlight that the ease of synthesis and low cost, coupled with multifunctional properties, make MFCMP-1 an attractive functional material in practical applications.

Introduction

Over the past few years, new classes of high surface area microporous organic polymers (MOPs) have attracted tremendous scientific attention owing to their diverse potential applications as functional materials.[1] Different from inorganic or inorganic-organic hybrid microporous materials such as zeolites and metal-organic frameworks (MOFs), the MOPs are assembled through strong carbon-carbon, carbon-nitrogen, and/or carbon-oxygen covalent bonds between organic building blocks. The rigid and contorted skeleton structures suppress the space-efficient packing in the solid state, such contributed to the permanent porosity. Interestingly, one of the most attractive aspects is the promise of tuning pore parameters and skeleton properties through rational structural design, intensive selection of organic building unites and synthetic techniques. Diverse synthesis strategies involving cross-coupling or self-condensation reactions have been employed to construct MOPs, and led to various kinds of novel porous materials, including crystalline covalent organic frameworks[2] and triazine-based organic frameworks,[3] as well as amorphous conjugated microporous polymers,[4] hyper-crosslinked polymers,[5] polymers of intrinsic microporosity,[6] element organic frameworks[7] and porous aromatic frameworks.[8] They have been demonstrated as functional porous materials for gas storage and separation, sensors, electronics and heterogeneous catalysts. Despite impressive progress in the area of MOPs, currently, the design and construct of functional microporous frameworks is also a preferential consideration.[9] Even more remarkably, these applications can be combined and integrated into an individual framework to form multifunctional MOP. However, up to now, the cost-effective and multifunctional microporous organic frameworks have not been reported.

Among various types of porous organic polymers, CMPs as a sub-family of MOPs combining π-conjugated skeleton and permanent micropores in one material, in sharp contrast to non-conjugated porous materials and conventional nonporous conjugated polymers. They have been demonstrated high potential for use in gas adsorption, light emitting, light harvesting and heterogeneous catalysis.[10] As useful platform, the CMPs would be constructed expediently to form the advanced multifunctional materials. It is well known that the performance of porous materials is determined crucially by the characters of building units. For design cost-effective and multifunctional microporous materials, our strategy is assembling a special functional monomer into the polymer with good π-conjugated and inherent microporous features by an inexpensive method. Recently, Han and co-workers have developed a facile method for construction of the conjugated microporous organic frameworks with excellent gas storage through carbazole-based oxidative coupling polymerization.[11] In this context, 2,4,6-tris(carbazolo)-1,3,5-triazine was widely studied as an excellent carrier transport and phosphorescent host material.[12] It is easily synthesized through commercial raw materials, and allowing large-scale preparation. In addition, its rigid conjugated backbone of polycarbozole is beneficial for formation of a porous framework with permanent microporousity and good physicochemical stability. With these considerations in mind, in

this contribution, we contribute a strategy for design and construct of a cost-effective multifunctional conjugated microporous polymer (MFCMP-1) based on a single carbazole-based monomer with excellent performances in gas storage, molecular sensing and solid catalysis. Abundant nitrogen atoms in skeleton, which may increase the interaction of adsorbent and small gas molecules, and high nitrogen active contents in pore wall lead still network to become a promising Lewis basic heterogeneous organocatalyst. In addition, high emission and three dimensional π-conjugated characteristics of framework facilitated rapid response and enhanced detection sensitivities for electron-deficient compounds. We further highlight that building a three-dimensional multifunctional CMP network by a cost-effective way, which is essential for the scale-up preparation of porous materials with potential applications.

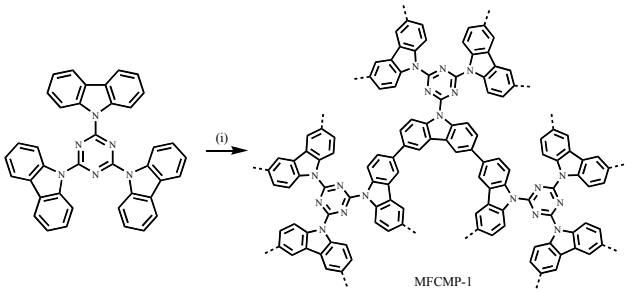

Scheme 1 Synthetic procedure to multifunctional carbazole-based conjugated microporous polymer (i) $FeCl_3/CHCl_3$

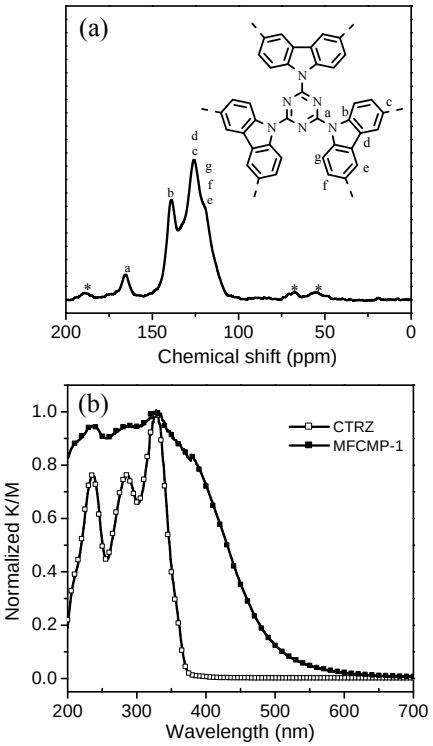

Fig. 1 (a) ^{13}C CP/MAS NMR spectrum of the MFCMP-1. Asterisks (*) indicate peaks arising from spinning side bands. (b) UV-spectra of MFCMP-1 and its monomer.

Results and discussion

$FeCl_3$-promoted oxidative polymerization of thienylene[13] or carbazole-based[11] building blocks exhibits cost-effective advantages in the construction of microporous organic polymers, such as inexpensive catalyst, facile reaction conditions and high yield. In particular, the single reactant is essential for scale-up preparation of porous materials with practical applications. Therefore, along this line, three-dimensional 2,4,6-tris(carbazolo)-1,3,5-triazine (CTRZ) building block containing three carbazole units was selected as the single monomer in this study, the oxidative polymerization was promoted by stoichiometric amount of anhydrous $FeCl_3$ under nitrogen atmosphere (Scheme 1). Different solvents including acetonitrile, acetonitrile/chloroform and chloroform in polymerization reaction were researched firstly, in order to achieve a high surface area for the resulting polymer frameworks. We can find that the polymerization reaction occurs immediately in chloroform under reflux, and the precipitation of a brown-dark solid is obtained. After polymerization, the polymer MFCMP-1 was washed carefully with methanol and concentrated HCl solution and was obtained in 96% yield followed by Soxhlet extraction with tetrahydrofuran for 24 h. The light-yellow powder has a low density and is insoluble in water or any common organic solvents. It is chemically stable, even exposed to dilute solution of acid and base, which suggested highly cross-linked and robust structures. The thermal stability of MFCMP-1 was characterized by thermogravimetric analysis and 5% mass loss was 310 ^oC under nitrogen (Fig. S1). The chemical composition and connectivity of the building blocks were investigated by spectra and analytical methods, which includes Fourier transform infrared (FT-IR), solid-state ^{13}C cross polarization magic angle spinning (CP/MAS) NMR and elemental analysis. The success of the cross coupling was first confirmed by FT-IR measurements. Fig. S2 showed FT-IR spectra of MFCMP-1 and its starting material. We can find that MFCMP-1 also retains some feature peaks of monomer, while more broadening profiles accord with the characteristics of the polymer. The structure of MFCMP-1 was characterized at the molecular level by ^{13}C solid state NMR. The ^{13}C CP-MAS NMR spectrum of the obtained polymer with the assignments of the resonances is shown in Fig. 1a. The low-intensity peak at 165.5 ppm is ascribed to the carbon atoms present in the triazine ring. The signal peak at 139.1 ppm can be ascribed to the substituted phenyl carbons binding with nitrogen atom. The high-intensity at 126.1 ppm is attributed to the signal of other substituted phenyl carbons. The resonance at 118.7 ppm is due to the unsubstituted phenyl carbons. The electronic adsorption spectra of MFCMP-1 exhibited a long tailing in the low energy region, which suggested an extended π-conjugation over the skeleton (Fig. 1b). Different from the crystalline covalent organic frameworks, powder X-ray diffraction (PXRD) profiles of MFCMP-1 did not show any sharp signals, which indicate that the polymer framework has an amorphous structure (Fig. S3). Scanning electron microscopy (SEM) images showed that MFCMP-1 adopted a plate-like morphology in the sub-micrometer scale (Fig. S4a). The size distribution of the polymer samples at room temperature in a methanol suspension was 91.4 ± 14.4 nm (Fig. S4b). High-resolution transmission electron microscopy (TEM) image revealed the presence of a porous texture (Fig. S4c). Additionally, no iron residues in the polymer could be detected by ICP measurement.

In order to characterize the porosity parameters of MFCMP-1, the nitrogen adsorption/desorption isotherm was measured at 77 K. As shown in Fig. 2a, the polymer exhibits a combination of type-I and II nitrogen sorption isotherm featured according to the IUPAC classification and shows a rapid nitrogen gas uptake at low relative pressure (0-0.1 bar), reflecting a permanent

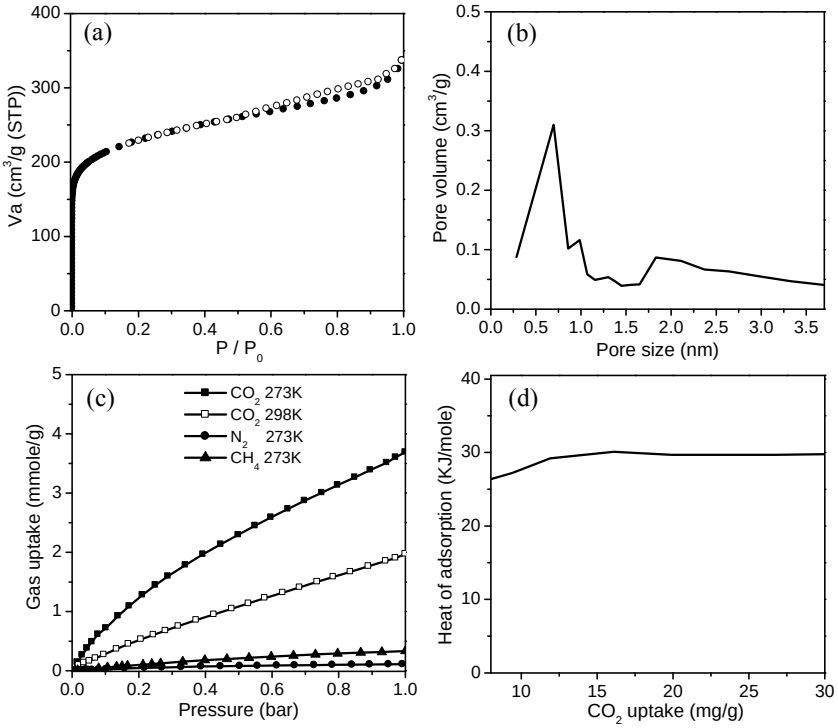

Fig. 2 (a) Nitrogen adsorption/desorption isotherms (●: adsorption, o: desorption). (b) Pore size distribution of MFCMP-1. (c) CO_2 (■ at 273 K, □ at 298 K), CH_4 (▲ at 273 K) and N_2 (● at 273 K) adsorption isotherm of MFCMP-1. (d) The isosteric heat of adsorption CO_2.

microporous nature of the network. The increase in the nitrogen sorption at a high relative pressure may arise in part due to interparticulate porosity associated with the meso/macrostructures of the samples. The specific surface areas were calculated in the relative pressure range from 0.01 to 0.1, and the results showed that the Brunauer–Emmett–Teller (BET) specific surface area of MFCMP-1 was 843 m^2 g^{-1}. The total volume calculated with nitrogen gas adsorbed at P/P_0 = 0.99 was 0.521 cm^3 g^{-1}, while the micropore volume calculated by the t-plot method was 0.239 cm^3 g^{-1} for MFCMP-1. Furthermore, MFCMP-1 has a wide pore size distribution with the pore widths centering around 0.69, 0.83 and 1.84 nm, respectively, as calculated by the Saito–Flory method (Fig. 2b).

Once the porosity of MFCMP-1 has been established, we considered firstly its application in gas uptake. Microporous material with a narrow pore distribution or abundant ultramicroporous components may interact attractively with small gas molecules through improved molecular interaction. Carbon dioxide capture or separation from flue gases or coal-fired plants is highly attractive owing to environmental and economical reasons.[14] Hence, CO_2 isotherms of MFCMP-1 were measured at 298 and 273 K (Fig. 2c). At 273 K and 1 bar pressure, the CO_2 adsorption was about 16.2 wt% (3.69 mmol g^{-1}) for MFCMP-1. In particular, the adsorption curve is gradually increasing, suggesting higher uptake capacity for carbon dioxide upon further enhancing the pressure. As can be seen, MFCMP-1 shows a higher carbon dioxide adsorption capacity than many reported MOPs[15] under the same conditions, such as lithium-loaded porous aromatic framework PAF-18-OLi (14.4 wt%, at 273 K, SA_{BET} = 981 m^2 g^{-1}),[16] nitrogen-rich microporous poly(benzimidazole) network TBI-1 (14.0 wt%, at 273 K, SA_{BET} = 609 m^2 g^{-1}),[17] nitrogen and oxygen-rich microporous polyimide

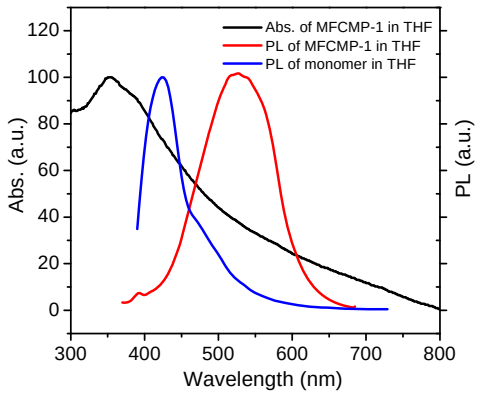

Fig. 3 UV-vis and the fluorescent emission spectra of MFCMP-1 and the fluorescent emission spectrum of CTRZ in THF.

network MPI-2 (13.8 wt%, at 273 K, SA_{BET} = 814 m^2 g^{-1}),[18] carbazole–spacer–carbazole conjugated network P-2 (14.5 wt%, at 273 K, SA_{BET} = 1222 m^2 g^{-1}).[19] However, the carbon dioxide uptake value of MFCMP-1 is lower than that of previously successful examples including carbazole-based porous organic polymer CPOP-1 (4.82 mmol g^{-1}, at 273 K, SA_{BET} = 2220 m^2 g^{-1},[11a] benzimidazole-linked polymers with higher surface areas[20] and imine-linked porous polymer framework PPF-1 (6.07 mmol g^{-1}, at 273 K, SA_{BET} = 1740 m^2 g^{-1}).[21] We think that the good adsorption performance could be attributed to the high surface area, large micropore volume of the polymer as well as the abundant nitrogen sites in the network. Indeed, MFCMP-1 not only shows the high CO_2 uptake, but also has the large isosteric

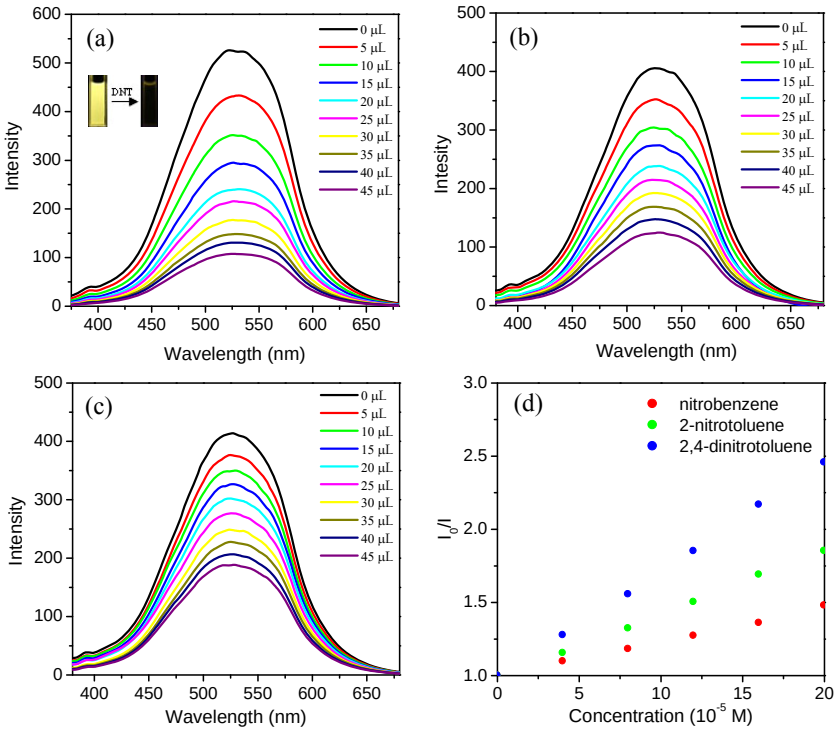

Fig. 4 The fluorescent emission spectra of the THF solutions of MFCMP-1 with different concentration of 2,4-dinitrotoluene (a), 4-nitrotoluene (b) and nitrobenzene (c). Stern-Volmer plots of MFCMP-1 upon titration with various arenes.

heat (Qst). As shown in Fig. 2d, the Qst for carbon dioxide is 30.1–25.9 KJ mol^{-1}, depending on the degree of carbon dioxide loading. This value is higher than values reported for many other MOPs,[15] possibly because of the relatively smaller pore size and higher nitrogen content of MFCMP-1. It well know that the electron-rich nitrogen atoms can yield strong dipole-quadrupole interaction with carbon dioxide, leading to a significant increase in adsorption parameters.[22] Carbon dioxide uptake was also tested at 298 K and 10 bar. The adsorption isotherm shown in Figure S5, which indicated that MFCMP-1 has a high uptake for carbon dioxide in this condition. In addition to the high uptake and reversibility, a good selectivity for CO_2 over N_2 and CH_4 is one of the necessary for a material to be used as a CO_2 adsorbent. The adsorption isotherms of CH_4 and N_2 at 273 K were measured and are compared with that of CO_2 in Figure 2c. The curves display that CO_2 has the considerably higher uptake than CH_4 and N_2 in the whole pressure range. On the basis of initial slope calculations in the pressure range of 0 to 0.1 bar, the ideal adsorption selectivity of CO_2/N_2 and CO_2/CH_4 is 31 and 14, respectively (Figure S6). Although the values are lower than those of some MOPs,[15,20b,23] they are comparable to many other types of polymers as well as porous carbon monoliths.[24] In addition, MFCMP-1 remains also a basic structure including connect and porosity after stirring for five hours in boiling water (Figure S7), which implying a practical application in the post-combustion CO_2 capture.

Similar to linear π-conjugated polymer, the three-dimensional MFCMP-1 exhibits good luminescent properties. MFCMP-1 has an adsorption band at 361 nm with a long tail in THF (Fig. 3). Furthermore, the photoluminescence (PL) spectrum of the MFCMP-1 dispersed in THF exhibits strong fluorescence with quantum yield of about 6.1%, and an emission band was observed at 529 nm upon excitation at 380 nm (Fig. 3). The fluorescence of the MFCMP-1 is completely different from that of its monomer, which gives a strong fluorescence peak at 425 nm (Fig. 3). This observed red-shift is likely due to good three dimensional π-conjugated character of polymer skeleton. Introducing luminescence and porosity into three-dimensional conjugated polymers are expected as an important design strategy for rapid detection of explosive compounds.[25] To explore the ability of MFCMP-1 to sense the nitroaromatic compounds,

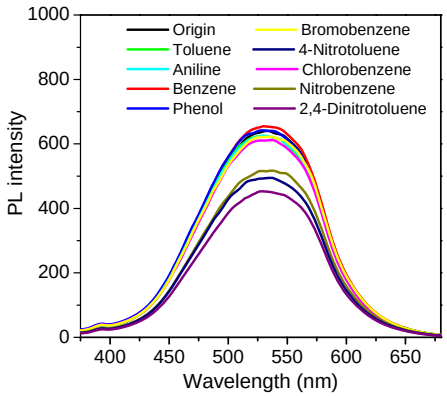

Fig. 5 The fluorescent emission spectra of the THF solutions of MFCMP-1 with 150 ppm of different analytes (excited at 380 nm).

fluorescence-quenching titrations were performed with the incremental addition of analytes to MFCMP-1 dispersed in THF. As shown in Fig. 4, in all sensing experiments, the fluorescence quenching efficiency increased drastically with the analyte

amount even in the low concentration range (<0.04 mM) and leveled off at high concentration to reach nearly complete quenching (>80%). Further, the fluorescence quenching efficiency was analyzed using the Stern-Volmer (SV) equation, $I_0/I = Ksv\ [A] + 1$, where I_0 is the initial fluorescence intensity before the addition of analyte, I_0 is the fluorescence intensity in the presence of analyte, [A] is the molar concentration of analyte, and Ksv is the quenching constant. The SV plots for 2,4-dinitrotoluene (DNT), 4-nitrotoluene (NT) and nitrobenzene (NB) were nearly linear at low concentrations and Ksv was 7.2×10^3, 4.3×10^3 and 2.3×10^3 M^{-1} for DNT, NT and NB, respectively, which are comparable to known organic polymers.[26] This general trend is in good agreement with the trend in reduction potentials of nitro-substituted compounds. Indeed, different electron deficient aromatics have different effects in the fluorescence intensity of the dispersed solution of MFCMP-1 in THF. The addition of a small amount of the analytes (150 ppm) into the dispersed solution of MFCMP-1, in sharp contrast with nitro-substituted aromatic compounds, other organic aromatic compounds such as benzene, toluene, phenol, aniline, chlorobenzene and bromobenzene have a negligible effect on the fluorescence intensity of MFCMP-1 (Fig. 5). These results imply that MFCMP-1 has a selective fluorescence response to nitroaromatic compounds. Because the nitro group is a typical electron-withdrawing substituent, we propose the fluorescence response with photoinduced electron transfer mechanism from MFCMP-1 to nitroaromatics, that is, in the presence of nitroaromatics, the excited electron of the MFCMP-1 would undergo a transfer to the analyte, instead of relaxation to the ground state with the fluorescence emission.[26a]

As a novel kind of high-performance heterogeneous catalysts and catalyst supports, the porous organic polymers have attracted extensive attention in recent years.[1e,1f,27] The heterogeneous catalysis can not only be able to avoid the leaching of noble metal but also overcome the difficulties for separating the soluble catalyst from the reaction system, which is the green, safe, and environmentally friendly process to produce fine chemicals. In particular, the development of metal-free heterogeneous organocatalysts is also an important challenge. Owing to high surface area, large pore volume, good thermal stability as well as rich nitrogen basic sites, MFCMP-1 would be highly expected as a cost-effective, atomic-efficient, recyclable solid organocatalyst.

It is well known that the Knoevenagel condensation by Lewis base is one of the most powerful and widely employed protocols for carbon-carbon bond formation in the synthesis of fine chemicals and pharmaceutical sciences. In the context, we investigated the Knoevenagel reactions as a model reaction to estimate the heterogeneous organocatalytic properties of MFCMP-1 network. We accordingly tested the Knoevenagel reactions of malononitrile with various types of aromatic aldehydes. The influence of different solvents, reaction time and catalyst uptake on the yield was firstly researched. As could be seen in Table S1, the dioxane, tetrahydrofuran (THF), toluene, dimethylformamide (DMF) and ethyl acetate proved to be poor solvents (4–8%, Table S1, entries 1–5), while H_2O, methanol and ethanol afforded moderate yields in the same condition (48, 41 and 65%, Table S1, entries 6–8). In sharp contrast, however, high yields were obtained in methanol/H_2O, ethanol/H_2O, DMF/H_2O and dioxane/H_2O at a 1:1 volume ratio which could be attributed to the good solubility of both organic reactants with those solvents (76–99%, Table S1, entries 9–12). In addition, the yields were decreased with reduced reaction time (Table S1, entries 13–16). No surprisingly, increasing molar ration of malononitrile/benzaldehyde can result in higher reaction rate (Table S1, entry 17). However, low catalytic activity was obtained upon a reduced amount of MFCMP-1, and product yield of 95% could be achieved in more than 7 h (Fig. 6a). For a reaction to be feasible for industrial application, a short reaction

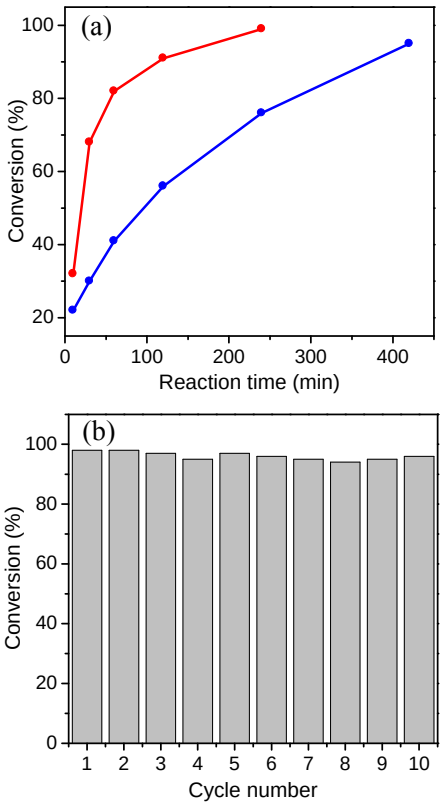

Fig. 6 (a) Comparison of catalytic activity of MFCMP-1 in the model reaction (●: 0.5 mol% of the substrate; ●: 1.0 mol% of the substrate) and (b) reusability of MFCMP-1 in the large-scale Knoevenagel reaction for the benzaldehyde (1.0 g) with malononitrile.

would be highly attractive. Therefore, the optimal reaction conditions were identified as follows: benzaldehyde (0.2 mmol), malononitrile (0.2 mmol), MFCMP-1 (1 mmol%) in dioxane/H_2O (0.4 mL/0.4 mL) at room temperature for 4 h. To explore the scope of the Knoevenagel condensation reaction by our system, the reactions of various aldehydes, including aromatic, heterocyclic aldehydes and cyclic ketone with malononitrile were investigated in the presence of MFCMP-1, and the results were summarized in Table 1. Substrates bearing different electron-donating and electron-withdrawing aldehydes were all efficiently transformed to show the corresponding unsaturated dinitrile products with good to excellent yields (Table 1). However, a slightly lower yield than that of reported catalytic systems was found, owing to the shorter reaction time and lower catalyst loading.[28] Indeed, a yield of 85% for **2i** could be achieved after 4h under the optimited conditions. Enhancing the catalyst concentration to 3.0 mol% of the substrate led to a significant improvement of the reaction rate with 94% conversion being achieved after 3 h (Table 1, entry 8). In addition, the reaction of heteroaromatic aldehydes with malononitrile gave expected product **2j** in excellent yields. Interestingly, double coupling took place with excellent yield when 2,5-Thiophenedicarboxaldehyde was used. In contrast to the reported porous polybenzimidazole networks,[29] the Knoevenagel reactions by MFCMP-1 network have rapid transformations with high yield, which attributed to

higher surface area and larger pore volume of the polymer framework. These results indicated that the MFCMP-1 network has a potential application in the Knoevenagel reactions.

We also examined the recyclability and organocatalytic stability of MFCMP-1 in the model reaction using benzadehyde and malononitrile as substrates. The recycling experiment was carried out by using a simple filtration method to recover the insoluble MFCMP-1. The recovered MFCMP-1 organocatalyst was then washed THF and acetone to remove the residual substrates and products, dried in vacuum overnight, reused in the next round of condensation reactions. The organocatalyst MFCMP-1 can be efficiently recycled and reused for ten repeating cycles without significant loss of catalytic activity and the original structure (Fig. 6b and S8), which attributed to the built-in nature of the covalently linked catalytic sites in skeleton. As such, the novel polymer MFCMP-1 has a promise as a high-efficient, recyclable, and low-cost solid organocatalyst.

Conclusions

In summary, we have synthesized a carbazole-based multifunctional conjugated microporous polymer via oxidative coupling polymerization method with cost-effective advantages. Owing to the combination of the inherent microporous, rich nitrogen activated sites and strong fluorescent emission, the polymer framework displays high adsorption capacity for carbon dioxide with good selectivity and acts as an efficient heterogeneous organocatalyst for the Knoevenagel condensation with high activity, widely substrate adaptability and good recyclability, leading to the formation of the C-C coupling products in excellent yields. Particularly, the luminescent emission of the polymer could be quenched efficiently by DNT, suggesting that it can serve as a sensitive chemosensor for explosive detection. Low cost and excellent performances make MFCMP-1 an attractive functional material in practical applications. Currently, the design and construction of new functional POPs for energy, environment and catalytic-related applications is underway in our laboratory.

Experimental section

Materials

Carbazole, cyanuric chloride, ferric chloride, BuLi and chlorobenzene were purchased from Aldrich and used as received. Other organic solvents for reactions were distilled over appropriate drying reagents under nitrogen. Deuterated solvents for NMR measurement were obtained from Aldrich.

Physical characterization

^{1}H spectra were recorded on a Varian Mercury-300 NMR spectrometer, where chemical shifts (δ in ppm) were determined with a residual proton of the solvent as standard. Matrix-assisted laser desorption ionization time-of-flight mass (MALDI-TOF MS) spectra were performed on an Applied Biosystems BioSpectrometry model Voyager-DE-STR spectrometer in reflector or linear mode using 9-nitroanthracene or dithranol as a matrix. Solid-state ^{13}C CP/MAS NMR measurement was recorded on a Bruker AVANCE III 400 WB spectrometer at a MAS rate of 5 kHz and a CP contact time of 2 ms. The infrared spectra were recorded from 400 to 4000 cm^{-1} on a Nicolet FT-IR 360 spectrometer by using KBr pellets. Field emission scanning electron microscopy was performed on a SU8020 model HITACHI microscope. Transmission electron microscopy was performed on a JEOL model JEM-2100 microscope. The sample was prepared by drop-casting a supersonicated methanol suspension of MFCMP-1 onto a copper grid. The Fe contents in polymer frameworks were determined by Perkin-Elmer ICP-OES

Table 1. The Knoevenagel condensation of various aldehydes with malononitrile catalyzed by MFCMP-1.[a]

Entry	Aldehydes	Product	Yield (%)[b]
1	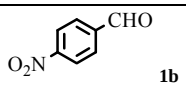 1b	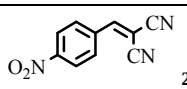 2b	93
2	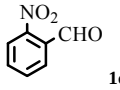 1c	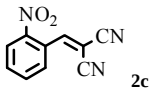 2c	95
3	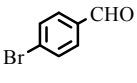 1d	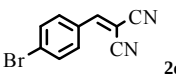 2d	88
4	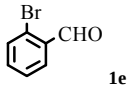 1e	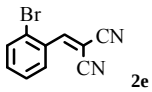 2e	87
5	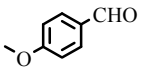 1f	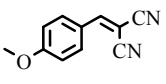 2f	94
6	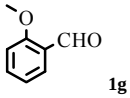 1g	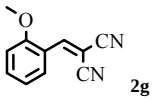 2g	98
7	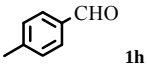 1h	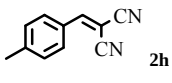 2h	89
8	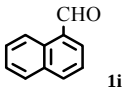 1i	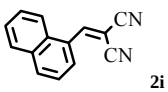 2i	85 94[c]
9	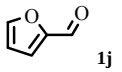 1j	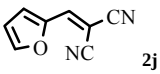 2j	98
10	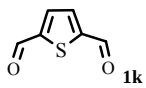 1k	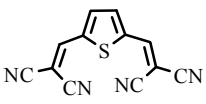 2k	88
11	 1l	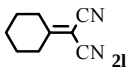 2l	91

[a] Rection conditions: aromatic aldehyde (0.2 mmol), malononitrile (0.2 mmol), MFCMP-1 (1.0 mol % of the substrate), dioxane (0.4 mL), H_2O (0.4 mL), 25 °C and 4 h. [b] Yield of the isolated product obtained after column chromatography. [c] MFCMP-1 (3.0 mol % of the substrate), 3 h.

Optima 3300DV spectroscopy. Powder X-ray diffraction data was recorded on a PANalytical BV Empyrean diffractometer by depositing powder on glass substrate, from $2\theta = 4.0°$ to 60° with 0.02° increment at 25 °C. Thermogravimetric analysis (TGA) was performed on a TA Q500 thermogravimeter by measuring the weight loss while heating at a rate of 10 °C min^{-1} from 25 to 800 °C under nitrogen. Nitrogen sorption isotherms were measured at 77 K with a JW-BK 132F analyzer. Before measurement, the samples were degassed in vacuum at 150 °C for more than 10 h. The Brunauer-Emmett-Teller (BET) method

was utilized to calculate the specific surface areas and pore volume, the Saito-Foley (SF) method was applied for the estimation of pore size distribution. The catalytic products were quantified by GC analysis (Shimadzu GC-2014C) under the following conditions: N_2 was used as a carrier gas at a flow rate of 1.0 mL min^{-1}. GC was conducted using a Rtx-5 column (30 m × 0.25 mm × 0.25 mm, Restek, USA). The injector-port temperature was set at 270 °C. The column temperature was programmed from 130 °C (5 min hold) to 280 °C at 50 °C min^{-1}, and keep the temperature for 5 min. Undecane was used as internal standard. GC-MS was performed using a QP2010 gas chromatography mass spectrometer (GC-2010 coupled with a GC-MS QP-2010, Shimadzu) equipped with a DB-5MS column (30 m × 0.25 mm × 0.25 μm, Agilent). The column temperature was programmed from 150 °C (2 min hold) to 280 °C at 50 °C min^{-1}. Mass spectra were obtained by electron-impact (EI) at 70 eV using the full-scan mode.

Synthesis of 2,4,6-Tricarbazolo-1,3,5-triazine (CTRZ) [30]

Carbazole (1.6 g, 9.65 mmol) was dissolved in dry THF (20 mL) under an argon atmosphere in a two-necked round-bottom flask. n-Buthyllithium (6.59 mL, 1.6 M in hexane solution) was added dropwise to the carbazole solution at –78 K and the mixture was stirred for 1 h at room temperature. The carbazole-lithium solution was added dropwise to the cyanuric chloride (0.5 g, 2.73mmol) solution using a transfer canula within 10 min. The reaction mixture was refluxed for 6 h. After the solution was cooled to room temperature, 20 mL of water were added. The product was filtered off, washed with water, hexane and diethyl ether. Pure product was obtained by extractive filtering with hot chlorobenzene through a short silica gel bed, recrystallizing repeatedly from the same solvent, and drying under a vacuum at 100 °C for 4 h to remove chlorobenzene, which was 0.8 g (51%) of a white solid. ^{1}H NMR (300 MHz, $CDCl_3$, δ): 7.45-7.48 (m, 12 H), 8.14 (d, 6H), 9.03 (d, 6H) ppm. MALDI-TOF MS: m/z 576.21, calcd. for $C_{39}H_{24}N_6$; found, $[M + H]^+$ 576.23.

Synthesis Procedure of Carbazole-Based MFCMP-1 Networks by Oxidative Coupling Polymerization:

All of the carbazole-based multifunctional conjugated microporous polymers were synthesized through $FeCl_3$-promoted oxidative coupling polymerization of monomer. The reaction was carried out in anhydrous chloroform, and found to maximize surface area in the microporous polymer frameworks. A typical experimental procedure for MFCMP-1 is given in details as follows: the monomer CTRZ (150 mg, 0.26 mmol) was dispersed in anhydrous chloroform (20 mL), and then transferred dropwise to a suspension of ferric chloride (675 mg, 4.1 mmol) in anhydrous chloroform (15 mL). The mixture was stirred for 3 day under nitrogen at 60 ^{o}C, and then 50 mL of methanol was added to the reaction mixture. The resulting mixture was kept stirring for another hour and the precipitate was collected by filtration. After being washed with methanol, the obtained solid was stirred vigorously in hydrochloric acid solution for 1 h. The suspension was then filtered and washed with water and methanol, and then extracted in a Soxhlet extractor with methanol and THF for 24 h. The target product was dried at 120 °C under vacuum for 24 h to give a yellow powder (yield: 96%). Different solvent systems (Chloroform/CH_3CN, and CH_3CN) in polymerization reaction were investigated, in order to achieve high surface areas for the resulting polymer frameworks. The isolation yields for MsMOP-1 obtained in various reaction conditions is 68% and 75%. The nitrogen sorption isotherms and pore distributions of MFCMP-1 in different reaction conditions were showed in Figure S9.

Acknowledgements

This work was supported by the National Natural Science Foundation of China (Nos.: 51203058, 51173061 and 21074043). X. Liu is also grateful for support by the Frontiers of Science and Interdisciplinary Innovation Project of Jilin University (No.: 450060481015).

Notes and references

[a] *State Key Laboratory for Supramolecular Structure and Materials, College of Chemistry, Jilin University, 2699 Qianjin Avenue, Changchun, 130012, P.R.China. E-mail: xm_liu@jlu.edu.cn*
[b] *State Key Laboratory of Inorganic Synthesis and Preparative Chemistry, College of Chemistry, Jilin University, Changchun, 130012, P.R.China.*
[c] *State Key Laboratory on Integrated Optoelectronics, College of Electronic Science and Technology, Jilin University, Changchun, 130012, P.R.China.*

† Electronic Supplementary Information (ESI) available: TGA, PXRD, UV, EDS, SEM and TEM images for MFCMP-1 samples, catalytic data, ^{1}H-NMR and GC-MS data for the catalytic products. see DOI: 10.1039/b000000x/

1 (a) R. Dawson, A. I. Cooper, D. J. Adams, *Prog. Polym. Sci.* 2012, **37** 530-563; (b) A. I. Cooper, *Adv. Mater.* 2009, **21**, 1291-1295; (c) A. Thomas, *Angew. Chem. Int. Ed.* 2010, **49**, 8328-*8344*; (d) N. B. McKeown, P. M. Budd, *Macromolecules* 2010, **43**, 5163-5176; (e) Y. Zhang, S. N. Riduan, *Chem. Soc. Rev.* 2012, **41**, 2083-2094; (f) P. Kaur, J. T. Hupp, S. B. T. Nguyen, *ACS Catal.* 2011, **1**, 819-835; (g) D. Wu, F. Xu, B. Sun, R. Fu, H. He, K. Matyjaszewski, *Chem. Rev.* 2012, **112**, 3959-4015.
2 (a) H. M. El-Kaderi, J. R. Hunt, J. L. Mendoza-Cortes, A. P. Cote, R. E.Taylor, M. O'Keeffe, O. M. Yaghi, *Science* 2007, **316**, 268-272; (b) J. W. Colson, W. R. Dichtel, *Nature Chem.* 2013, **5**, 453-465; (c) X. Feng, X. S. Ding, D. L. Jang, *Chem. Soc. Rev.* 2012, **41**, 6010-6022; (d) S. Y. Ding, W. Wang, *Chem. Soc. Rev.*, 2013, **42**, 548-568.
3 (a) P. Kuhn, M. Antonietti, A. Thomas, *Angew. Chem., Int. Ed.* 2008, **47**, 3450-3453; (b) P. Kuhn, A. Forget, J. Hartmann, A. Thomas, M. Antonietti, *Adv. Mater.* 2009, **21**, 897-901; (c) X. M. Liu, H. Li, Y. W. Zhang, B. Xu, S. G. A, H. Xia, Y. Mu, *Polym. Chem.* 2013, **4**, 2445-2448.
4 (a) J. X. Jiang, F. Su, A. Trewin, C. D. Wood, N. L. Campbell, H. Niu, C. Dickinson, A. Y. Ganin, M. J. Rosseinsky, Y. Z. Khimyak, A. I. Cooper, *Angew. Chem., Int. Ed.* 2007, **46**, 8574-8578; (b) J. Weber, A. Thomas, J. *Am. Chem. Soc.* 2008, **130**, 6334-6335; (c) X. M. Liu, S. G. A, Y. W. Zhang, X. L. Luo, H. Xia, H. Li, Y. Mu, *RSC Adv.*, 2014, **4**, 6447-6453; (d) X. Liu, Y. Xu, Z. Guo, A. Nagai, D. L. Jiang, *Chem. Commun.*, 2013, **49**, 3233-3235; (e) S. G. A, Y. W. Zhang, Z. P. Li, H. Xia, M. Xue, X. M. Liu and Y. Mu. *Chem. Commun.,* 2014, DOI: 10.1039/C4CC01783H.
5 (a) J. Y. Lee, C. D. Wood, D. Bradshaw, M. J. Rosseinsky, A. I. Cooper, *Chem. Commun.* 2006, 2670-2672; (b) B. Y. Li, R. N. Gong, W. Wang, X. Huang, W. Zhang, H. M. Li, C. X. Hu, B. E. Tan, *Macromplecules* 2011, **44**, 2410-2414; (c) M. G. Schwab, A. Lennert, J. Pahnke, G. Jonschker, M. Koch, I. Senkovska, M. Rehahn, S. Kaskel, *J. Mater. Chem.* 2011, **21**, 2131-2135.
6 (a) N. B. McKeown, P. M. Budd, *Chem. Soc. Rev.* 2006, **35**, 675-683; (b) N. B. McKeown, B. Gahnem, K. J. Msayib, P. M. Budd, C. E. Tattershall, K. Mahmood, S. Tan, D. Book, H. W. Langmi, A. Walton, *Angew. Chem. Int. Ed.* 2006, **45**, 1804-1807; (c) M. Carta, R. Malpass-Evans, M. Croad, Y. Rogan, J. C. Jansen, P. Bernardo, F. Bazzarelli and N. B. McKeown, *Science* 2013, **339**, 303-307.
7 (a) M. Rose, W. Böhlmann, M. Sabo, S. Kaskel, *Chem. Commun*. 2008, 2462-2464; (b) J. Fritsch, F. Drache, G. Nickerl, W. Böhlmann, S. Kaskel, *Micropor. Mesopor. Mater.* 2013, 172, 167-173; (c) X. M. Liu, Y. W. Zhang, H. Li, S. G. A, H. Xia, Y. Mu, *RSC Adv.* 2013, **3**, 21267-21270.
8 T. Ben, H. Ren, S. Ma, D. Cao, J. Lan, X. Jing, W. Wang, J. Xu, F. Deng, J. M. Simmons, S. Qui, G. Zhu, *Angew. Chem., Int. Ed.* 2009, **48**, 9457-9460.

9 J. X. Jiang, C. Wang, A. Laybourn, T. Hasell, R. Clowes, Y. Z. Khimyak, J. Xiao, S. J. Higgins, D. J. Adams, A. I. Cooper, *Angew. Chem., Int. Ed.* 2011, **50**, 1072-1075.

10 Y. H. Xu, S. B. Jin, H. Xu, A. Nagai, D. L. Jiang, *Chem. Soc. Rev.* 2013, **42**, 8012-8031; (b) A. Li, R. F. Lu, Y. Wang, X. Wang, K. L. Han, W. Q. Deng, *Angew. Chem., Int. Ed.* 2010, **49**, 3330-3333; (c) A. Li, H. X. Sun, D. Z. Tan, W. J. Fan, S. H. Wen, X. J. Qing, G. X. Li, S. Y. Li, W. Q. Deng, *Energy Environ. Sci.* 2011, **4**, 2062-2065; (d) Y. Xie, T. T. Wang, X. H. Liu, K. Zou, W. Q. Deng, *Nat. Commun*. 2013, **4**, 1960.

11 (a) Q. Chen, M. Luo, P. Hammershoj, D. Zhou, Y. Han, B. W. Laursen, C. G. Yan, B. H. Han, *J. Am. Chem. Soc.* 2012, **134**, 6084-6087; b) Q. Chen, D. P. Liu, M. Luo, L. J. Feng, Y. C. Zhao, B. H. Han, *Small* 2014, **10**, 308-315.

12 H. Inomata, K. Goushi, T. Masuko, T. Konno, T. Imai, H. Sasabe, J. J. Brown, C. Adachi, *Chem. Mater.* 2004, **16**, 1285-1291.

13 (a) S. Yuan, S. Kirklin, B. Dorney, D. J. Liu, L. Yu, *Macromolecules* 2009, **42**, 1554-1559; (b) J. Schmidt, J. Weber, J. D. Epping, M. Antonietti, A. Thormas, *Adv. Mater.* 2009, **21**, 702-705.

14 Q. A. Wang, J. Z. Luo, Z. Y. Zhong, A. Borgna, *Energy Environ. Sci.* 2011, **4**, 42-45.

15 (a) R. Dawson, A. I. Cooper, D. J. Adams, *Polym. Int.* 2013, **62**, 345-352; (b) Y. C. Zhao, T. Wang, L. M. Zhang, Y. Cui and B. H. Han, *ACS Appl. Mater. Interfaces*, 2012, **4**, 6975-6981; (c) Q. Chen, J. X. Wang, F. Yang, D. Zhou, N. Bian, X. J. Zhang, C. G. Yan, B. H. Han, *J. Mater. Chem.* 2011, **21**, 13554-13560.

16 H. P. Ma, H. Ren, X. Q. Zou, F. X. Sun, Z. J. Yan, K. Cai, D. Y. Wang, G. S. Zhu, *J. Mater. Chem. A* 2013, **1**, 752-758.

17 Y. C. Zhao, Q. Y. Cheng, D. Zhou, T. Wang, B. H. Han, *J. Mater. Chem.* 2012, **22**, 11509-11514.

18 G. Y. Li, Z. G. Wang, *Macromolecules* 2013, **46**, 3058-3066.

19 S. Q. Qiao, Z. K. Dua, R. Q. Yang, *J. Mater. Chem. A,* 2014, **2**, 1877-1885.

20 (a) M. G. Rabbani, H. M. El-Kaderi, *Chem. Mater.* 2011, **23**, 1650-1653; (b) M. G. Rabbani, H. M. El-Kaderi, *Chem. Mater.* 2012, **24**, 1511-1517; (c) M. G. Rabbani, T. E. Reich, R. M. Kassab, K. T. Jackson, H. M. El-Kaderi, *Chem. Commun.* 2012, **48**, 1141.

21 Y. L. Zhu, H. Long, W. Zhang, *Chem. Mater.* 2013, **25**, 1630-1635.

22 R. Babarao, S. Dai, D. E. Jiang, *Langmuir* 2011, **27**, 3451-3460.

23 L. Liu, P. Z. Li, L, L. Zhu, R. Q. Zou, Y. L. Zhao, *Polymer* 2013, **54**, 596-600.

24 (a) A. Laybourn, R. Dawson, R. Clowes, J. A. Iggo, A. I. Cooper, Y. Z. Khimyak, D. J. Adams, *Polym. Chem.* 2012, **3**, 533-3-537; (b) G. P. Hao, W. C. Li, D. Qian, G. H. Wang, W. P. Zhang, T. Zhang, A. Q. Wang, F. Schüth, H. J. Bongard, A. H. Lu, *J. Am. Chem. Soc.* 2011, **133**, 11378-11388.

25 (a) X. Liu, Y. Xu, D. Jiang, *J. Am. Chem. Soc.* 2012, **134**, 8738-8741; (b) J. L. Novotney, W. R. Dichtel, *ACS Macro Lett.* 2013, **2**, 423-426; (c) L. B. Sun, Z. Q. Liang, J. H. Yu, R. R. Xu, *Polym. Chem.* 2013, **4**, 1932-1938.

26 (a) S. Shanmugaraju, H. Jadhav, R. Karthikb, P. S. Mukherjee, *RSC Adv.* 2013, **3**, 4940-4950; (b) J. Li, J. Z. Liu, J. W. Y. Lama, B. Z. Tang, *RSC Adv.* 2013, **3**, 8193-8196.

27 H. Li, B. Xu, X. M. Liu, S. G. A, C. Y. He, Y. Mu, *J. Mater. Chem. A* 2013, **1**, 14108-14114.

28 (a) D. Z. Xu, Y. J. Liu, S. Shi, Y. M. Wang, *Green Chem.* 2010, **12**, 514-517; (b) S. H. Z hao, X. J. Wang, L. W. Zhang, *RSC Adv.* 2013, **3**, 11691-11696; (c) A. Dhakshinamoorthy, M. Opanasenko, J. Cejla, H. Garcia, *Adv. Synth. Catal.* 2013, **355**, 247-268; (d) Q. R. Fang, S. Gu, J. Zheng, Z. B. Zhuang, S. L. Qiu, Y. S. Yan, *Angew. Chem., Int. Ed* 2014, **53,** 2878-2882.

29 (a) P. Makowski, J. Weber, A. Thomas, F. Goettmann, *Catal. Commun.* 2008, **10**, 243-247; (b) X. J. Zhang, N. Bian, L. J. Mao, Q. Chen, L. Fang, A. D. Qi, B. H. Han, *Macromol. Chem. Phys.* 2012, **213**, 1575-1581.

30 M. M Rothmann, S. Haneder, E. D. Como, C. Lennartz, C. Schildknecht, P. Strohriegl, *Chem. Mater.* **2010**, *22*, 2403-2410.

A multifunctional conjugated microporous polymer exhibits a combination of functionalities such as selective CO_2 uptake, sensor for hazardous and explosive molecules and highly efficient heterogeneous catalysis.